equilibrium between the free stream and the region of minimum pressure. The result is

$$T = \frac{4\sigma}{3r_e}\left[3\left(1+\frac{p_o - p_v}{2\sigma / r_e}\right)\right]^{-1/2} \tag{7-12}$$

where p_o is the pressure when the equilibrium radius is r_e.

Eq. (7-12) implies that the critical pressure for cavitation inception approaches vapor pressure, p_v, when there is a sufficient supply of nuclei greater than approximately 100 microns. When the number of sufficiently large nuclei is small, the pressure required for cavitation inception can be negative; that is, the flow is locally in tension as described by Eq. (7-12).

Measured ranges of nuclei size distributions are shown in Figure 7-13. The sizes are presented in the form of number density (number of nuclei per unit volume in a given size range, m^{-4}) versus nuclei size in microns. Because the total number of nuclei per unit volume is the integral of number density over the entire nuclei size range, simple dimensional arguments suggest that the number density, n, is proportional to r^{-4}. This power law is also sketched in Figure 7-13. The data are for two water tunnels, whose nuclei are mostly microbubbles, and for two other facilities (a water tunnel and a depressurized towing tank) whose nuclei consist mostly of solid particles. The data indicate that nuclei population that are dominated by micro-bubbles sensitive to the relative saturation level of dissolved gas.

The size ranges in Figure 7-13 also indicate that a reasonable number of larger bubbles exist in most facilities (when liquid tensions are less than 5 kPa). However, there is evidence that the flow field around a given body produces a screening effect such that larger bubbles tend to move out of the critical-pressure region leaving only smaller bubbles with more negative critical pressures to be active in the cavitation process. Very little has been done to investigate the question of the influence of nuclei size distribution on cavitation. What information exists indicates that this question can be important for interpreting results from models.

The question of an adequate distribution of nuclei in a modeling facility is important for modeling developed cavitation as well as determining cavitation-inception limits. This is especially true for unsteady cavitation, such as vibration due to cavitation on a propeller operating in a nonuniform inflow.

Techniques for the measurement of cavitation nuclei have been developed over the past 30 years. A coherent review of nuclei measurement is given by Billet (1985). It is only recently that reliable measurements have become possible. Most methods of nuclei measurement are tedious and require sophisticated equipment. The venturi technique—originally sug-

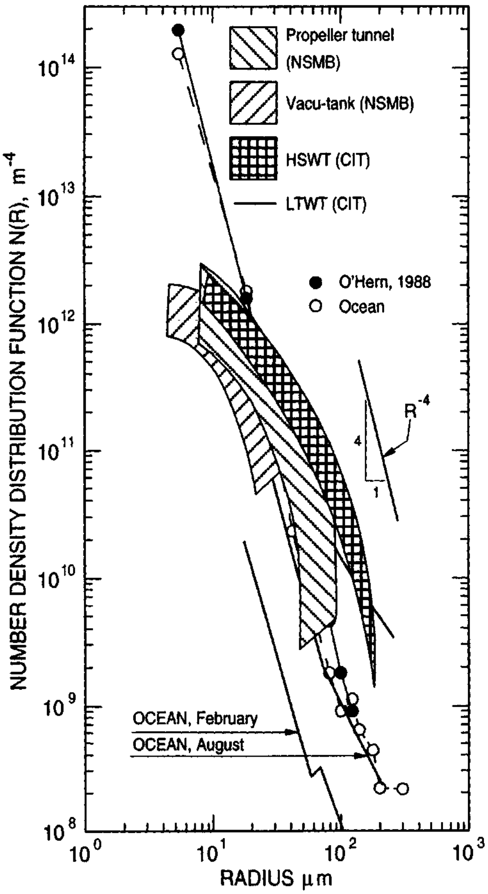

FIGURE 7-13. Measured ranges of nuclei size distributions.

Note: Data for propeller tunnel (NSMB) and Vacu-tank (NSMB) are from Arndt and Keller 1976; data for HSWT (CIT) and LTWT (CIT) are from Gates and Acosta 1978; data for OCEAN, February and August, are from Medwin 1977; and data for • and ° are from O'Hern 1987.

gested by Oldenziel (1982) and improved by several other investigators, notably d'Agostino and Acosta (1991a,b), LeGoff and LeCoffre (1983), and Keller (1987)—shows promise for monitoring the cavitation susceptibility of test water on a relative basis. Holography or phase-Doppler anemometry show the most promise for quantitative measurements of nuclei size.

7.6.4 Influence of Dissolved Gas

The bubble dynamics of vaporous cavitation have been described above. Noncondensible gas in solution can also play a role in vaporous cavitation, since the size and number of nuclei in the flow are related to the concentration of dissolved gas (see Figure 7-13).

Under certain circumstances, cavitation can occur when the lowest pressure in a flow is substantially higher than vapor pressure. In this case, bubble growth is attributable to diffusion of dissolved gas across the bubble wall. This can occur when nuclei are subjected to pressures below the saturation pressure for a relatively long period of time. Holl (1960) suggested that gaseous cavitation can occur when the flow is locally supersaturated. He suggested an equilibrium theory such that

$$(p_\infty - p_v)_c \leq p_s = \beta C_g \tag{7-13}$$

where

p_s = saturation pressure,
β = Henry's constant, and
C_g = concentration of dissolved gas.

Subscript c implies cavitation conditions may occur. Henry's constant is a function of the type of gas in solution and the water temperature. As a rule of thumb β = 6,700 Pa/ppm for air, when concentration is expressed in a mole/mole basis. In other words, water is saturated at one atmosphere when the concentration is 15 ppm. Thus, for gaseous cavitation an upper limit on Ca_i is

$$Ca_i = (-C_p)_{\min} + \frac{\beta C_g}{0.5\rho U_o^2} \tag{7-14}$$

Holl's (1960) experiments indicate that both types of cavitation occur in the same experiment. This is an important consideration when examining trends produced by hydraulic-model data. The two types of cavitation result from different physical processes and it is sometimes difficult to distinguish between them. Taghavi and Arndt (1985) suggest the classification given in Table 7-3 for distinguishing between vaporous and gaseous cavitation. It should be noted that dissolved gas may influence measured values of hydrodynamic loads in cavitating flows (Arndt 1981a,b).

7.6.5 Facilities and Techniques

Most cavitation observations and measurements are made using models placed in special laboratory facilities. The exception to this is the recent development of cavitation monitoring techniques for hydroturbines, as

TABLE 7–3. Features Distinguishing Gaseous Cavitation and Vaporous Cavitation.

Gaseous Cavitation	Vaporous Cavitation
High dissolved air content	Low dissolved air content
Low velocities	High velocities
Small cavitation bubbles, uniform in size, and distributed evenly	Disparate vapor pockets
Cushioned cavitation noise pulses	High-strength noise pulses
Cavitation number, *Ca*, decreases with velocity as $1/U^2$	*Ca* mildly increases with, or is independent of, velocity

described by Abbot and Lowell (1991), for example. Typical laboratory facilities include:

- water tunnels,
- depressurized flumes and depressurized towing tanks,
- pump and turbine test loops, and
- cavitation erosion test apparatus.

Water Tunnels. Water tunnels have been used for a wide variety of cavitation testing and research for about a century. The first known use of a water tunnel for cavitation research is attributed to Parsons in 1895 (Young 1990). Since that time these facilities have grown in size and complexity. As of 1995, the largest facility of this kind is the U.S. Navy Large Cavitation Channel (Wetzel and Arndt 1994a,b).

A typical water tunnel is shown in Figure 7-14, which is of the recirculating type. Important features necessary for cavitation tests include accurate, stable, and independent control of pressure and velocity; measurement equipment for velocity, pressure, temperature, dissolved gas content, and nuclei content and control; and photographic and video equipment. Because of the unsteady nature of cavitation and the extremely rapid physical processes that occur during bubble collapse and erosion, many laboratories are equipped with highly specialized high-speed video and photographic cameras that are capable of very high framing rates. The latest in video equipment is capable of framing rates as high as 40,500 frames per second.

Free-Surface Facilities. A variety of facilities have been developed for studying cavitation phenomena in free-surface flows. These include water tunnels with a variable pressure, free-surface test section, like the one shown in Figure 7-15, and specialized variable-pressure towing tanks for

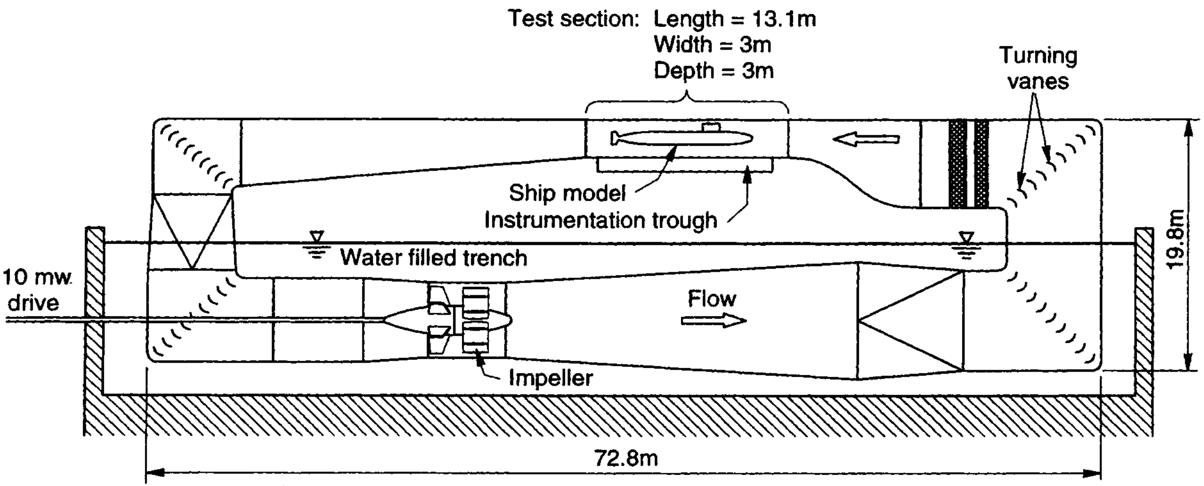

FIGURE 7-14. Recirculating water tunnel operated by the David Taylor Model Basin of the U.S. Navy.

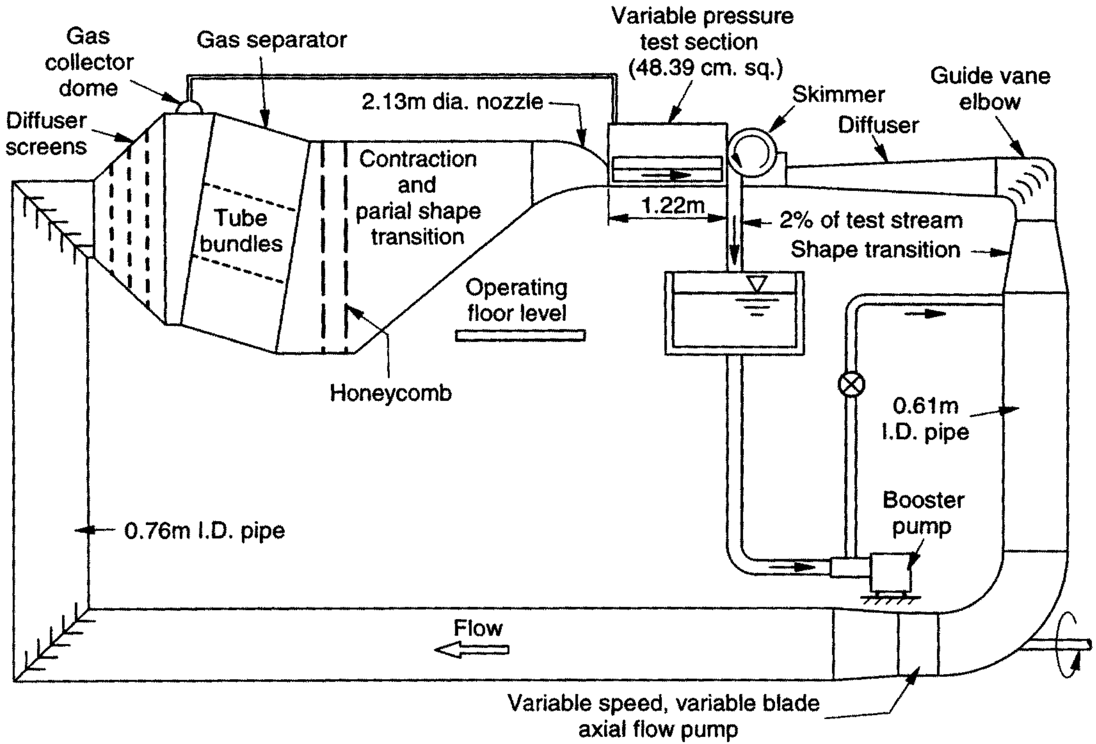

FIGURE 7-15. Schematic of variable pressure, free-surface water tunnel at the St. Anthony Falls Hydraulics Laboratory.

model tests with ship hulls. The International Towing Tank Conference (ITTC 1995) gives an extensive inventory of such facilities.

It is important to note that cavitation testing in free-surface flows can be especially demanding in terms of pressure control. Simultaneous modeling of cavitation number and Froude number requires scaling of the free-surface pressure in accordance with

$$(p_o - p_v)_r = X_r = Y_r \tag{7-15}$$

where X is horizontal scale and Y is vertical scale.

For example, tests with a 25:1-scale model would have to be carried out at a pressure of approximately 1/25 of an atmosphere. Few convenient facilities are available for such modeling. Mefford (1984), though, describes incipient cavitation studies conducted using the Bureau of Reclamation's 17 m^3, low-ambient-pressure chamber, which operates in a pressure range of 1.0 to 0.1 atmosphere. Note that, with few exceptions, geometric distortion should not be used for cavitation modeling.

Pump and Turbine Test Loops. Pump and turbine test loops are similar in concept to water tunnels. Model testing is an important element in the design and development phases of turbine manufacture (see Chapter 11). Most laboratories equipped with model turbine test stands are owned by manufacturers. However, there are independent laboratories available where relative performance evaluations between competing manufacturers can be carried out. All test loops perform basically the same function. Section 11.6 describes the operation of a typical turbine test loop. For investigating turbine cavitation, a model turbine is driven by high-pressure water from a head tank and discharges into a tail tank, as shown in Figure 11-1. The flow is recirculated by a pump, usually positioned well below the elevation of the model to ensure cavitation-free performance of the pump while performing cavitation testing with the turbine model. One important advantage of a recirculating turbine test loop is that cavitation testing can be done over a wide range of cavitation indices at constant head and flow.

Cavitation Erosion Test Facilities. In many cases, the service life of equipment and hydraulic structures subject to cavitation erosion can range from months to years. Because of the relatively lengthy periods required to observe measurable erosion in the field, many different techniques have been developed in the laboratory to achieve significant time compression. The time compression factor achieved in accelerated erosion tests can be as high as 10^5 (Durrer 1986).

Many of the devices used have little relationship to actual field conditions. For this reason, they have been typically used for screening tests of different types of materials especially susceptible to cavitation erosion. Recent research is aimed at relating screening tests to predictions of service life in various applications (Arndt et al. 1995).

The most commonly used device is the ASTM vibratory apparatus. An oscillating horn produces a periodic pressure field that induces the periodic growth and collapse of a cloud of cavitation bubbles. A sample placed at the tip of the horn or immediately below it is easily eroded. The standard frequency of operation is 20 kHz, which produces a very high erosion rate on account of the rapid recycling of the cavitation process. New methods are being developed for measuring erosion rates at full scale. Usually erosion rate is inferred from the measurement of noise or vibration.

7.7 EXAMPLES

Two examples are presented: first, gas–liquid flow with four significant forces acting and, second, spillway cavitation. The examples briefly illustrate different aspects of gas–liquid flow modeling. The first is an inquiry into bubble-rise processes. The second example focuses on the problem of cavitation at a specific dam spillway.

7.7.1 A Gas–Liquid Flow with Four Significant Forces

The dynamic similitude problem created by the presence of four forces (gravity, inertia, surface tension, and viscosity) can be clearly demonstrated by ascending large air bubbles (slug flow) in long vertical tubes, as shown by the correlations in Figure 7-3. In recent experiments conducted at Georgia Institute of Technology, the rise of large air bubbles was studied using four liquids (water, ethylene glycol, white oil, and glycerol) in precision-bore glass tubes ranging in diameter from 6 mm to 25 mm. The experiments were designed such that the each of four forces could play a role over certain ranges of parameters. Figure 7-16 illustrates the correlation of the Froude number, *Fr*, in terms of the Eötvos number, *Eö*, for the four values of the Property number, *Pn*, for the four liquids. From these data (unpublished at the time this Manual was being written), and from the more extensive results plotted from White and Beardmore (1962) and from Wallis (1969), the following conclusions can be made.

1. Standing bubbles of zero velocity correspond to a balance of gravity and surface tension, giving a constant value of $E\ddot{o} = 3.37$.
2. For water, many aqueous solutions, and other low-viscosity fluids, bubble motion is governed solely by inertia and surface tension for $3.37 < E\ddot{o} < 100$, independent of liquid viscosity.

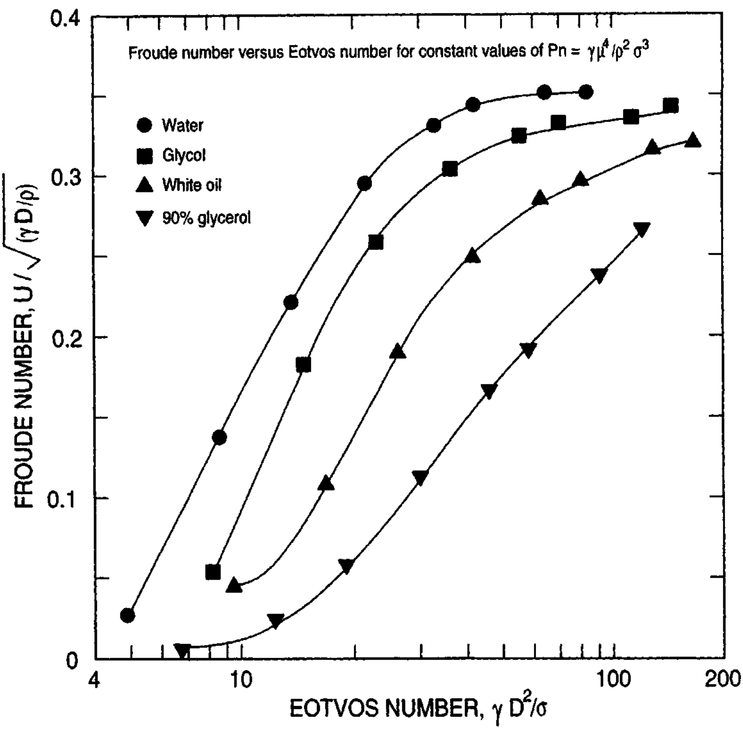

FIGURE 7-16. Example of dynamic similitude with comparable effects of surface tension, viscosity, and inertia in glass tubes.

3. For *Eö* > 200, and high Reynolds numbers, Taylor bubbles exist and reflect a balance between inertia and gravity forces, yielding a constant value $Fr = 0.35$.
4. Over the remainder of Figure 7-16, all four forces contribute to varying degrees.

7.7.2 Spillway Cavitation

As an example of hydraulic model tests, the test setup for specialized cavitation testing of the spillway of Guri Dam in Venezuela is shown in Figure 7-17. A view of the cavitation damage to the prototype spillway is depicted in Figure 7-11. The model, described by Ripken and Dahlin (1972), was built at a scale of 197:1 in a flume and operated in accordance with similitude of cavitation index, Eq. (7-6). The model provided design information about the causes of the cavitation and means to avoid it.

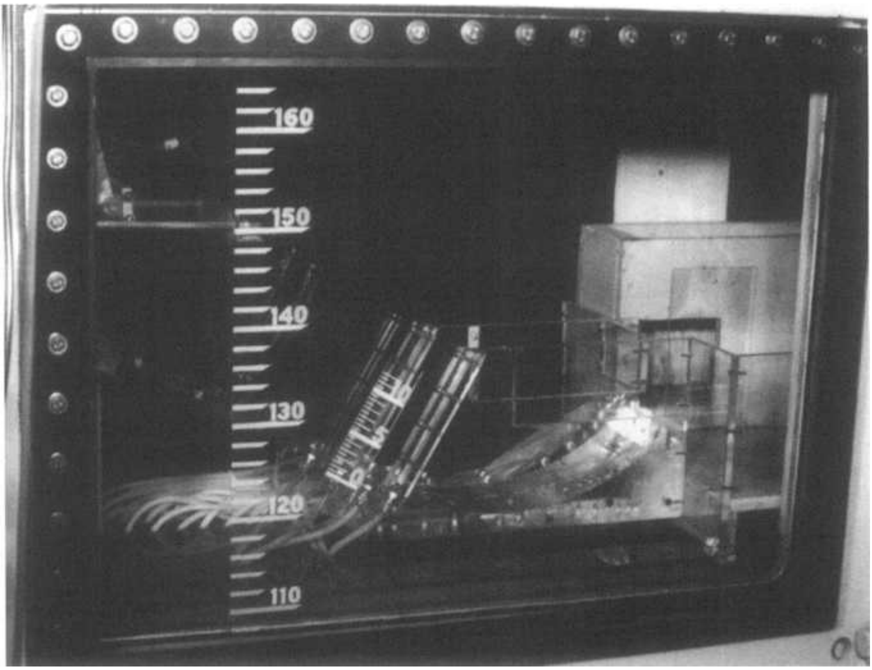

FIGURE 7-17. Test setup for cavitation testing of Guri Dam, Venezuela. The spillway is located within the water tunnel facility shown in Figure 7-15.